Room temperature ALD impact on efficiency, stability and surface properties in perovskite solar cells

Malgorzata Kot,*[a] Chittaranjan Das,[a] Zhiping Wang,[b] Karsten Henkel,[a] Konrad Wojciechowski,[b] Henry J. Snaith,[b] and Dieter Schmeisser[a]

Abstract: In this work, solar cells with a fresh-made $CH_3NH_3PbI_3$ perovskite film have shown power conversion efficiency (*PCE*) of 15.4%, while the one with 50 days aged perovskite film only 6.1%. However, when the aged perovskite was covered with a room temperature atomic layer deposited (ALD) Al_2O_3 the *PCE* value was clearly enhanced. X-ray photoelectron spectroscopy study has shown that the ALD precursors are chemically active only at the perovskite surface passivating it. Moreover, the ALD-Al_2O_3-covered perovskite films have shown enhanced ambient air stability.

Organic-inorganic perovskites[1-9] such as methylammonium lead halides ($CH_3NH_3PbX_3$, where X = I, Br, Cl) have emerged as very attractive absorber materials for the fabrication of low-cost and highly-efficient solar cells. However, a delicate nature of perovskite films may limit their practical applications. It is well known that hybrid perovskite films are prone to degradation in presence of moisture and oxygen within a couple of hours or days.[10-12] Moreover, the methylammonium lead triiodide ($CH_3NH_3PbI_3$) films cannot sustain prolonged annealing at temperatures higher than 85°C.[13,14] With the presence of moisture it also undergoes degradation upon applying electric field.[15] Enhancing the stability of the perovskite materials and devices against environmental degradation[16,17] is of great importance.

Atomic layer deposition (ALD) method has recently gained increased attention in the perovskite solar cell community.[16,18-21] ALD for highly controlled thin film deposition has been proven to be commercially viable for the largest scale manufacturing in multi-crystalline silicon photovoltaic for the passivated emitter rear cell (PERC), highlighting the feasibility of using this technique in perovskite technologies.[22] Conformal, dense and pinhole-free films can be achieved by ALD at very low temperatures (400°C – down to room temperature (RT)).[23-26] Concerning perovskite solar cells for example, an optimal ultra-thin ALD-processed Al_2O_3 buffer layer is capable to suppress carrier recombination and improve device efficiency.[19] Al_2O_3 as an encapsulating layer would increase moisture resistance of perovskite films and thus retard water-induced degradation.[21]

The lowest temperature reported so far to prepare Al_2O_3 using ALD method for the perovskite solar cell is equal to 70°C.[21] However, as mentioned earlier, long-time annealing of the perovskite films even at this low temperature would accelerate their degradation.[13,14] RT-ALD technique is hence highly desirable for Al_2O_3-based protection.

[a] Dr. M. Kot , Dr. C. Das, Dr. Karsten Henkel and Prof. Dr. D. Schmeisser
Applied Physics and Sensors
Brandenburg University of Technology Cottbus-Senftenberg
K.-Wachsmann-Allee 17, D-03046 Cottbus, Germany
E-mail: malgorzata.sowinska@b-tu.de

[b] Dr. Zhiping Wang, Dr. Konrad Wojciechowski and Prof. Dr. Henry J. Snaith
Clarendon Laboratory, University of Oxford,
Parks Road, Oxford OX13PU, United Kingdom

In this study, we use a RT-ALD technique to prepare a thin layer of Al_2O_3 on top of the aged perovskite film and investigate its impact on the solar cells performance and ambient air stability of the perovskite film itself. To correlate the electrical characterization results with the chemical and electronic properties of the RT-ALD-Al_2O_3/$CH_3NH_3PbI_3$ interface we perform a synchrotron- and laboratory-based X-ray photoelectron spectroscopy (SR-(XPS)) study. Our results indicate that the solar cells efficiency can be enhanced by performing only few cycles of trimethylaluminium (TMA) and H_2O precursors on the aged $CH_3NH_3PbI_3$ surface at RT. This is based on the fact that the ALD at RT only passivates the perovskite surface but the film bulk is not affected. Moreover, the thin layer of RT-ALD-Al_2O_3 enhances the perovskite film stability in ambient air conditions.

Firstly, solar cells containing either a fresh-made, or an unprotected-aged or a RT-ALD-Al_2O_3-protected-aged perovskite film are prepared and electrically characterized by current density – voltage (*J-V*) measurements. The final device structure is Ag/Spiro-OMeTAD/(RT-ALD-Al_2O_3)/perovskite/TiO_2/FTO/glass. The power conversion efficiency (*PCE*), stabilized power output (*SPO*), short circuit current (J_{SC}), open circuit voltage (V_{OC}) and fill factor (*FF*) values extracted from the *J-V* characteristics of all devices are shown in Figure 1 and are also summarized in Table 1. The fresh-made, non-aged perovskite solar cells without RT-ALD-Al_2O_3 film (gray points in Figure 1) exhibit a *PCE* value of 15.4±1.9%, which is comparable to our previous studies[27], suggesting the trustable quality of the perovskite films. However, the *PCE* of the aged perovskite solar cells without RT-

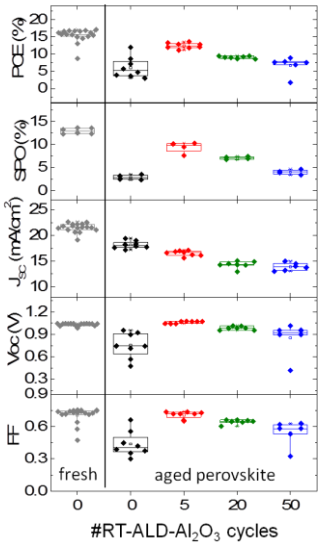

Figure 1. Photovoltaic performance of the fresh (gray points), unprotected-aged (black points) and Al_2O_3-protected-aged (No. of ALD cycles: 5 – red, 20 – green, and 50 – blue points) $CH_3NH_3PbI_3$ perovskite solar cells measured under simulated (AM1.5, 100 $mWcm^{-2}$) solar irradiation. The device structure is Ag/Spiro-OMeTAD/(RT-ALD-Al_2O_3)/perovskite/TiO_2/FTO/glass.

Table 1. Summarized parameters (power conversion efficiency (*PCE*), stabilized power output (*SPO*), short circuit current (J_{SC}), open circuit voltage (V_{OC}) and fill factor (*FF*)) of the perovskite solar cells containing fresh and covered with different number (#) of ALD cycles of Al_2O_3 aged perovskite films.

sample	#ALD cycles	*PCE* (%)	*SPO* (%)	Jsc ($mAcm^{-2}$)	Voc (V)	*FF*
fresh	0	15.4±1.9	12.9±0.6	21.5±0.8	1.04±0.02	0.71±0.07
aged	0	6.1±2.8	2.9±0.5	18.2±0.7	0.75±0.16	0.44±0.11
	5	12.4±0.8	9.4±1.1	16.5±0.5	1.05±0.01	0.71±0.03
	20	9.1±0.3	7.1±0.3	14.3±0.6	0.98±0.02	0.64±0.02
	50	6.8±2.3	4.0±0.5	13.9±0.7	0.85±0.20	0.54±0.10

ALD-Al_2O_3 film (black points in Figure 1) drops almost three times to 6.1±2.8%. Accordingly to Ref. [28], we attribute this *PCE* decrease to the chemical decomposition of the $CH_3NH_3PbI_3$ film. Nonetheless, in comparison to the unprotected-aged devices, the perovskite solar cells containing aged perovskite covered with RT-ALD-Al_2O_3 using different number of cycles (5 (red), 20 (green) and 50 (blue) in Figure 1) show relatively higher efficiencies in overall. Devices where five RT-ALD-Al_2O_3 cycles were performed achieve the champion *PCE* value of 12.4±0.8% and *SPO* of 9.4±1.1%. With further increasing number of RT-ALD-Al_2O_3 cycles, the overall device performance gradually decreases; however, it is still higher than the performance of the unprotected-aged devices. We notice that despite having obvious higher V_{OC} and *FF* the aged devices with RT-ALD-Al_2O_3 layer have a lower J_{SC} than the aged one without Al_2O_3 film. It is possible that the water vapor used in ALD might partially react with perovskite films resulting in lowering the device performance. Another possible reason for the reduced current density is that the holes generated in the perovskite film have to tunnel through the Al_2O_3 layer due to the deep valence band of Al_2O_3.[29]

In order to investigate the quality of the RT-ALD-Al_2O_3 layer and its effect on the perovskite solar cells performance we study the Al_2O_3/$CH_3NH_3PbI_3$ surface and interface by high energy resolution and surface sensitive synchrotron-based XPS study. In Figure 2 we show the Al2p (a) and O1s (b) SR-XPS data collected on the fresh-made, non-aged (0-ALD-Al_2O_3) and Al_2O_3 covered (5, 20 and 50 RT-ALD-Al_2O_3 cycles) perovskite films. As expected, in the as-prepared $CH_3NH_3PbI_3$ film there is no aluminum signal observable in the Al2p XPS region (Figure 2(a), black lines). However, in the O1s XPS spectrum a peak with the binding energy of 532.7 eV is already visible. Upon RT-ALD-Al_2O_3 cycles on perovskite film this peak and a second one at 531.1 eV arise along increasing number of ALD cycles. Both components intensity increases with increased number of ALD cycles, however, the peak at 531.1 eV increases much faster than the one at 532.7 eV as illustrated in the fitted O1s XPS spectra of the 20 (green components) and 50 (blue components) ALD cycles samples in Figure 2(b). Moreover, in the Al2p region also two peaks appear after ALD. One is located at 74.8 eV and the other one at 75.8 eV. The intensity of the one at 75.8 eV does not raise much along increasing number of ALD cycles. In agreement with literature[30], the peaks at 531.1 eV and at 74.8 eV, and at 532.7 eV and 75.8 eV are related to each other and are attributed to Al_2O_3 and (Al)-OH, respectively. Due to the difference of the kinetic energy of the photoelectrons originating from Al2p (higher kinetic energy = more bulk sensitive) and O1s (lower kinetic energy = more surface sensitive) levels we can conclude that the OH groups are present only at the film surface (initially at the perovskite, then at the ALD film surface) and that both the Al_2O_3 film thickness and the Al-OH concentration at the film surface are increasing with increased number of ALD cycles.

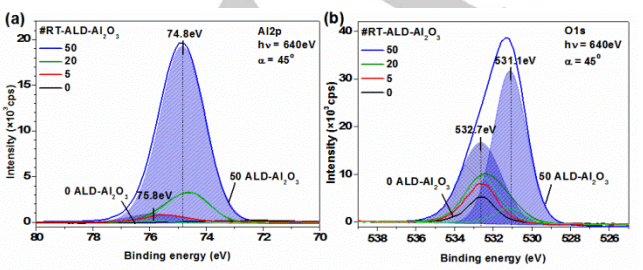

Figure 2. High energy resolution synchrotron-based X-ray photoelectron spectroscopy data of Al2p (a) and O1s (b) core levels of the as-prepared (marked with 0 ALD-Al_2O_3) and Al_2O_3 covered $CH_3NH_3PbI_3$ perovskite film (5, 20 and 50 ALD cycles) investigated using photons with energy of 640 eV and photoelectron take-off angle of 45°.

In Figure 3(a) we show the valence band (VB) spectra of the as-prepared and RT-ALD-Al_2O_3 covered perovskite film. Initially, for the as-prepared perovskite film the valence band maximum (VBM) is located at approximately 1.5 eV below Fermi level. Upon covering that film with the RT-ALD-Al_2O_3 layer we can observe accordingly a decrease of the I5p and a rise of the O2p peak. In the 20 ALD-Al_2O_3 cycles spectrum the VB shape shows a mixture of the $CH_3NH_3PbI_3$ and Al_2O_3. We note that, the VBM of the perovskite film with 5 and 20 ALD-Al_2O_3 cycles on it shifts towards lower binding energy by around 100 meV. This VBM shift could be caused by the interaction of perovskite film and aluminum precursor. After deposition of 50 ALD-Al_2O_3 cycles the VB is dominated by the Al_2O_3 emission and its VBM is located at 3.3 eV. A schematic diagram of the VB edge position with 5 and 50 ALD cycles is presented in Figure 3(b) and Figure 3(c) respectively. The band bending at the interface is very small for 5 ALD-Al_2O_3 due to a small (100 meV) VBM shift in perovskite. However, the perovskite and 50 ALD-Al_2O_3 interface has a downward band bending (Figure 3(c)) which limits the flow of photogenerated holes into the electrode and results in reduced *Jsc* value.

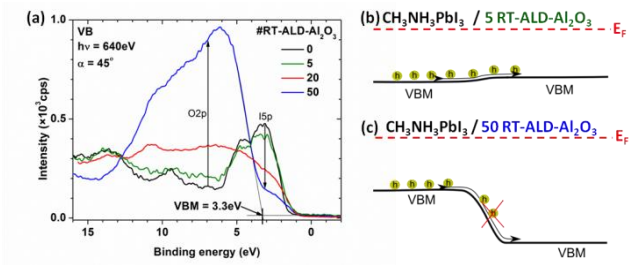

Figure 3. (a) High energy resolution synchrotron-based X-ray photoelectron spectroscopy data of valence band region of the as-prepared (0 – black) and Al_2O_3 covered $CH_3NH_3PbI_3$ perovskite film with increasing number (5 – green, 20 – red, and 50 – blue line) of ALD cycles investigated by using photons with energy of 640 eV and photoelectron take-off angle of 45°. Schematic band diagram of the perovskite/ALD film interface with 5 (b) and 50 (c) ALD cycles.

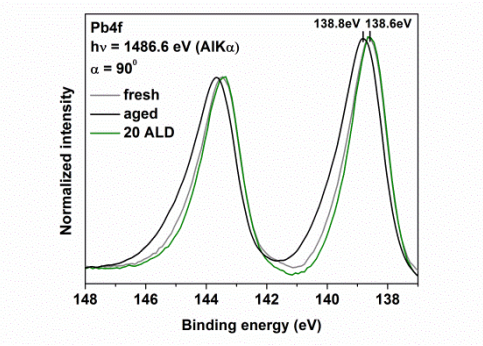

Figure 4. Normalized X-ray photoelectron spectroscopy data of the Pb4f core level of the fresh-made (gray line), aged (black line) and RT-ALD-Al_2O_3 covered with 20 ALD cycles (20 ALD, green line) perovskite film investigated using AlKα photons source with energy of 1486.6 eV at photoelectron take-off angle of 90°.

In order to verify if the perovskite bulk is influenced by the ALD precursors we have performed a laboratory-based XPS study of the Pb4f core level using AlKα radiation source at take-off angle of 90° (Figure 4) which allowed us to increase the information depth from 3.2 nm to approximately 9.4 nm below the film surface. By comparing the Pb4f XPS spectra of the as-prepared (fresh, gray line) and degraded (aged, black line) perovskite film (optical change from dark brown to yellow color, refer to Fig. 5) we can see that the Pb4f XPS peak is shifted towards higher binding energy and its full width at half maximum is increased. This Pb4f shift towards higher binding energy[31] and its broadening[28] for degraded perovskite films are in agreement with literature and attributed to the $CH_3NH_3PbI_3$ film decomposition to PbI_2. In contrast, the Pb4f shape and its binding energy do not change significantly after depositing 20-RT-ALD-Al_2O_3 film on the fresh perovskite film (20 ALD, green line). Therefore, it can be concluded that the ALD precursors are reacting only with the perovskite surface and they do not influence its bulk properties.

Typically, the as-prepared perovskite films are dark brown in color and gradually turn into yellow color after degradation due to the decomposition of $CH_3NH_3PbI_3$ into volatile CH_3NH_3I and PbI_2.[19] In order to verify if the RT-deposited Al_2O_3 film is a good barrier film for the perovskite material, the as-prepared $CH_3NH_3PbI_3$ perovskite film and those covered with 10 and 20 ALD cycles of Al_2O_3 were closed in plastic boxes filled with 20 ml of air of 50% humidity and stored for five months at RT. The result of the stability test is shown in Figure 5. After storing all samples in the same conditions the perovskite film without Al_2O_3 layer changed completely its color to yellow, whereas the one covered with 10 RT-ALD-Al_2O_3 cycles is partially turned to yellow and the one with 20 RT-ALD-Al_2O_3 cycles remains dark brown. This result indicates that by covering the $CH_3NH_3PbI_3$ perovskite film with an ultrathin Al_2O_3 layer one can significantly increase its resistance against moisture degradation.

Figure 5. Pictures of the fresh, as well as of the unprotected (0 ALD) and RT-ALD-Al_2O_3-protected (10 ALD and 20 ALD) $CH_3NH_3PbI_3$ perovskite film after five months of storing them in closed plastic boxes filled with 20 ml of ambient air with 50% humidity.

Our *J-V* results show that by covering the aged perovskite film with a RT-ALD-Al_2O_3 layer (even up to 50 ALD cycles) the *PCE* of the solar cells can be clearly enhanced. A double *PCE* enhancement from 6.1±2.8% for the non-protected sample (0 ALD) to 12.4±0.8% for the 5 ALD cycles sample has been achieved. It is noted that with increasing number of the ALD cycles this value is gradually decreasing. XPS characterization reveals that the ALD precursors are only chemically active at the RT-ALD-Al_2O_3/$CH_3NH_3PbI_3$ interface and the perovskite bulk is not changed. The TMA precursor interacts firstly rather with the OH groups present on the perovskite surface than with the H_2O vapor and with increasing number of the ALD cycles the OH groups are suppressed from the ALD/perovskite interface toward ALD surface. We speculate that the observed *PCE* enhancement for the first five ALD cycles may be thus related to the self-cleaning process[30] of the perovskite surface. However, during increasing number of ALD cycles we increase the Al_2O_3 thickness. Thicker film results in more bulk-like behavior including also higher band offsets and thus the holes created in the perovskite film have to tunnel through a thicker film and due to lower tunnel probability their flow is consequently reduced what is reflected in the smaller J_{SC} values. Moreover, we have seen that the perovskite film stability in ambient air is improved with a RT-ALD-Al_2O_3 adlayer. Most of the highly efficient perovskite solar cells are employing Spiro-OMeTAD combined with the use of lithium bis-trifluoromethanesulfonimide (Li-TFSI) dopant. Due to its hygroscopic nature, Li-TFSI can absorb H_2O easily, resulting in degradation of perovskite films. A thin layer of Al_2O_3 layer blocks thus the incorporation of H_2O absorbed by the Spiro-OMeTAD and in turn limits the degradation of the perovskite.

In summary, we have demonstrated that the perovskite solar cell performance and its stability can be improved by covering the perovskite film with a thin Al_2O_3 layer grown at RT by ALD. We relate the improvement of the V_{OC} and *FF* values during initial RT-ALD-Al_2O_3 cycles to the self-cleaning process which in effect decreases the series resistance between perovskite and hole transporting layer. A decrease of the *PCE* value with increasing number of ALD cycles is mainly caused by the decrease of J_{SC} which we link to the deep VBM for thicker Al_2O_3 films. Future directions will focus to optimize the Al_2O_3 film thickness and the ALD process parameters and to investigate the long-term stability of the perovskite solar cells with and without RT-ALD-Al_2O_3. Moreover, to get more insides on the role of OH groups on the perovskite solar cells performance we plan to replace the oxygen source to the water-free oxygen plasma[32].

Experimental Section

$CH_3NH_3PbI_3$ perovskite films were fabricated on a fluorine-doped tin oxide (FTO) coated glass (Pilkington, TEC7) accordingly to the recipe shown in Ref. 27. A perovskite precursor solution of the concentration of 400 mg/ml (CH_3NH_3I and $PbCl_2$, 3:1 molar ratio, in dimethylformamide (DMF, C_3H_7NO)) was spin-coated at room temperature (RT), followed by drying at RT for 30 min and annealing at 90°C for 150 min, and 120°C for 15 min. After that, the samples were closed separately in vacuum packs filled with nitrogen gas and stored in the glovebox. No additional cleaning procedure was applied. The Al_2O_3 films were deposited on the perovskite film at RT by ALD using trimethylaluminium (TMA) and water (H_2O) vapour as aluminium and oxygen precursors and nitrogen (N_2) as a purge gas. One complete ALD cycle consisted of 0.5 s of TMA, 2 × 0.5 s of N_2, 0.5 s of H_2O and 2 × 0.5 s of N_2 pulses. The pressure in the ALD

chamber was in the range of 1×10^{-5} mbar. The growth rate per cycle for ALD was found to be 0.14nm/cycles.

Perovskite films were prepared on the TiO_2/FTO/glass structure and stored for 50 days in the glove box with water level of 50 ppm. Then, these aged films were covered by Al_2O_3 film using different number of ALD cycles. To complete the solar cell structure, non-aged (fresh-made), unprotected-aged and Al_2O_3-protected-aged perovskite films were covered by Spiro-OMeTAD layer and Ag top electrode right before the *J-V* measurements.

Current density-voltage (*J-V*) characteristics of the Ag/2,2',7,7'-Tetrakis-(N,N-di-4-methoxyphenylamino)-9,9'-spirobifluorene (Spiro-OMeTAD)/(RT-ALD-Al_2O_3)/perovskite/compact TiO_2/FTO/glass solar cells were measured under AM1.5 light at 100 W/cm^2 generated using an ABET Class AAB sun 2000 simulator at a scan rate of 0.38 Vs^{-1} with a Keithley 2400 source meter.

Synchrotron-based X-ray photoelectron spectroscopy (SR-XPS) study was conducted at the undulator beamline U49/2-PGM2[33] at BESSY-II in Berlin/Adlershof with the ASAM end-station[34]. The photoelectrons were excited by X-rays with energies of 640 eV and recorded by the PHOIBOS-150 (SPECS GmbH) hemispherical electron analyzer equipped with a 1D delay line detector at take-off angle (α) of 45°.

Laboratory-based XPS study was conducted by using AlKα radiation source (1486.6 eV, Specs GmbH). The excited photoelectrons were collected by the hemispherical electron analyzer (Omicron) at α of 90°. The pressure in the main chamber during the measurement was better than 1×10^{-9} mbar.

The corresponding information depths (IDs) of the (SR-)XPS measurements (three times electron inelastic mean free path (λ) multiplied by sinα) calculated for the electron originating from the Pb4f level (binding energy 138.8 eV) and going through an Al_2O_3 matrix, using the TPP-2M formula from Ref. 35, are equal to 3.2 nm and 9.4 nm for the excitation energies of 640 eV (α = 45°) and 1486.6 eV (α = 90°), respectively.

Acknowledgement: Authors would like to acknowledge the support of Guido Beuckert from BTU. This work was partially supported by the German Research Foundation (DFG, SCHM 745/31-1), and by EPSRC, UK.

Keywords: perovskite solar cells • Al_2O_3 • ALD • XPS • stability

[1] H.-S. Kim, C.-R. Lee, J.-H. Im, K.-B. Lee, T. Moehl, A. Marchioro, S.-J. Moon, R. Humphry-Baker, J.-H. Yum, J. E. Moser, M. Grätzel, N. G. Park, *Sci. Rep.* **2012**, *2*, 591.

[2] M. M. Lee, J. Teuscher, T. Miyasaka, T.N. Murakami, H. J. Snaith, *Science* **2012**, *338*, 643.

[3] J. Burschka, N. Pellet, S.-J. Moon, R. Humphry-Baker, P. Gao, M. K. Nazeeruddin, M. Gratzel, *Nature* **2013**, *499*, 316.

[4] G. Hodes, Science **2013**, *342*, 317.

[5] C. Roldán-Carmona, O. Malinkiewicz, A. Soriano, G. Mínguez Espallargas, A. Garcia, P. Reinecke, T. Kroyer, M. I. Dar, M. K. Nazeeruddin, H. J. Bolink, *Energy Environ. Sci.* **2014**, *7*, 994.

[6] K. Wojciechowski, M. Saliba, T. Leijtens, A. Abate, H. J. Snaith, *Energy Environ. Sci.* **2014**, *7*, 1142.

[7] O. Malinkiewicz, A. Yella, Y. H. Lee, G. Minguez Espallargas, M. Graetzel, M. K. Nazeeruddin, H. J. Bolink, *Nature Photonics* **2014**, *8*, 128.

[8] J. Emara, T. Schnier, N. Pourdavoud, T. Riedl, K. Meerholz, S. Olthof, *Adv. Mater.* **2016**, *28,* 553.

[9] K. Wojciechowski, T. Leijtens, S. Siprova, C. Schlueter, M. T. Hörantner, J. T.-W. Wang, C.-Z. Li, A. K.-Y. Jen, T.-L. Lee, H. J. Snaith, *J. Phys. Chem. Lett.* **2015**, *6*, 2399.

[10] T. Leijtens, G. E. Eperon, S. Pathak, A. Abate, M. M. Lee, H. J. Snaith, *Nat. Commun.* **2013**, *4*, 2885.

[11] J. A. Christians, R. C. M. Fung, P. V. Kamat, *J. Am. Chem. Soc.* **2014**, *136*, 758.

[12] J. A. Christians, P. A. Miranda Herrera and P. V. Kamat, *J. Am. Chem. Soc.* **2015**, *137*, 1530.

[13] B. Conings, J. Drijkoningen, N. Gauquelin, A. Babayigit, J. D'Haen, L. D'Olieslaeger, A. Ethirajan, J. Verbeeck, J. Manca, E. Mosconi, F. D. Angelis, H.-G. Boyen, *Adv. Energy Mater.* **2015**, *5*, 1500477.

[14] L.-C. Chen, C.-C. Chen, J.-C. Chen, C.-G. Wu, *Solar Energy* **2015**, *122*, 1047.

[15] T. Leijtens, T. T. Hoke, G. Grancini, D. J. Slotcavage, G. E. Eperon, J. M. Ball, M. D. Bastiani, A. R. Bowring, N. Martino, K. Wojciechowski, M. D. McGehee, H. J. Snaith, A. Petrozza, *Adv. Energy Mater.* **2015**, *5*, 1500962.

[16] G. Niu, W. Li, F. Meng, L. Wang, H. Dong, Y. Qiu, *J. Mater. Chem. A* **2014**, *2*, 705.

[17] T. Leijtens, G. E. Eperon, N. K. Noel, S. N. Habisreutinger, A. Petrozza, H. J. Snaith, *Adv. Energy Mater.* **2015**, *5*, 1500963.

[18] C.-Y. Chang, K.-T. Lee, W.-K. Huang, H.-Y. Siao, Y.-C. Chang, *Chem. Mat.* **2015**, *27*, 5122.

[19] H. Si, Q. Liao, Z. Zhang, Y. Li, X. Yang, G. Zhang, Z. Kang, Y. Zhang, *Nano Energy* **2016**, *22*, 223.

[20] D. Choudhury, G. Rajaraman, S. K. Sarkar, *Nanoscale* **2016**, *8*, 7459.

[21] X. Dong, X. Fang, M. Lv, B. Lin, S. Zhang, J. Ding, N. Yuan, *J. Mater. Chem. A* **2015**, *3*, 5360.

[22] R. Sastrawan, D. Pysch, M. Bijker, F. Delahaye, B. Dielissen, W. Eipert, X. Gay, R. Görtzen, A. Hoffmann, B. Latzel, M. Lenes, X. Mao, S. Patzig-Klein, X.Qu, B. Sander, C. Schmitt, F. M. M. Souren, A. Träger, K. Weise, S. Yang and H. Nussbaumer, *Implementation of a multicrystalline ALD-Al_2O_3 PERC-technology into an industrial pilot production*, In proceedings of the 28th European Photovoltaic Solar Energy Conference and Exhibition, 2013, Paris, France, p. 1861.

[23] C. Das, K. Henkel, M. Tallarida, D. Schmeißer, H. Gargouri, I. Kärkkänen, J. Schneidewind, B. Gruska, M. Arens, *J. Vac. Sci. Technol. A.* **2015**, *33*, 01144.

[24] M. Sowińska, K. Henkel, D. Schmeißer, I. Kärkkänen, J. Schneidewind, F. Naumann, B. Gruska, H. Gargouri, *J. Vac. Sci. Technol. A* **2016**, *34*, 01127.

[25] S. Alberton Corrêa, S. Brizzi, D. Schmeisser, *J. Vac. Sci. Technol. A* **2016**, *1*, 01117.

[26] M. Sowinska, S. Brizzi, C. Das, I. Kärkkänen, J. Schneidewind, F. Naumann, H. Gargouri, K. Henkel, D. Schmeißer, Appl. Surf. Sci. **2016**, *381*, 42–47.

[27] G. E. Eperon, V. M. Burlakov, P. Docampo, A. Goriely, H. J. Snaith, *Adv. Funct. Mater*. **2013**, *24*, 151.

[28] W. Huang, J. S. Manser, P. V. Kamat, Sylwia Ptasinska, Chem. Mater. **2016**, *28*, 303.

[29] L. Zheng, Y. Ma, S. Chu, S. Wang, B. Qu, L. Xiao, Z. Chen, Q. Gong, Z. Wu, X. Hou, *Nanoscale* **2014**, *6*, 8171.

[30] M. Tallarida, K. Kukli, M. Michling, M. Ritala, M. Leskel and D. Schmeisser, *Chem. Mater*. **2011**, *23*, 3159.

[31] R. Lindblad, D. Bi, B.-W. Park, J. Oscarsson, M. Gorgoi, H. Siegbahn, M. Odelius, E. M. J. Johansson, H, Rensmo, J. Phys. Chem. Lett. **2014**, *5*, 648.

[32] K. Henkel, H. Gargouri, B. Gruska, M. Arens, M. Tallarida, D. Schmeißer, *J. Vac. Sci. Technol. A* **2014**, *32*, 01A107.

[33] D. Schmeißer, P. Hoffmann and G. Beuckert, Materials for Information Technology, edited by E. Zschech, C. Whelan, and T. Mikolajick (Springer, New York, 2005), 449.

[34] D. R. Batchelor, R. Follath and D. Schmeißer, Nuclear Instruments and Methods in Physics Research Section A, Accelerators, Spectrometers, Detectors and Associated Equipment, 467-468(1-2), 470 (2001).

[35] S. Tanuma, C. J. Powell, D. R. Penn, *Surf. Interface Anal.* **2003**, *35*, 239.

MANUSCRIPT

COMMUNICATION

Improved perovskite film stability in ambient air and solar cell power conversion efficiency by covering a perovskite film with a thin Al_2O_3 layer prepared by atomic layer deposition at room temperature are shown.

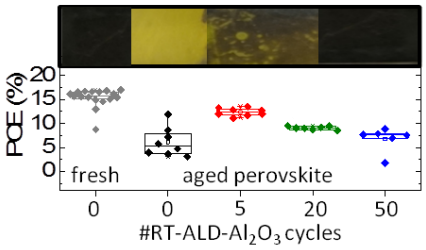

Dr. Malgorzata Kot, Dr. Chittaranjan Das, Dr. Zhiping Wang, Dr. Karsten Henkel, Dr. Konrad Wojciechowski, Prof. Dr. Henry J. Snaith and Prof. Dr. Dieter Schmeisser

Page No. – Page No.

Room temperature ALD impact on efficiency, stability and surface properties in perovskite solar cells

WILEY-VCH